EFFECT OF TEMPERATURE VARIATION ON HIGH TEMPERATURE FATIGUE OF MILD STEEL

S. Shimizu*, T. Mochizuki** and T. Fujimitsu*

INTRODUCTION

In the last decade, much research on high temperature fatigue of metals has been done. Most of the research focused on thermal fatigue [1-2] and the problem of rest in the midst of run [3-4]. In our studies we concentrated on the effect of temperature variation in fatigue of mild steel and we developed a new method of expression of results.

Andō et al. [5] and Dunsby [6] attempted fatigue tests by varying temperatures up and down; МАЛВКЕВИУ et al. [7] changed temperature conditions periodically; Katō et al. [8-9] carried out a series of experiments examining the correlation between strengthening and hardening as a result of "cyclic strain aging" [10]; Taira et al. [11] studied the effect of temperature variations on low-cycle fatigue life and we also conducted experiments relating to temperature variation [12-13].

In general, carbon steel exhibits higher fatigue strength at mildly elevated temperature than at room temperature (R.T.), the temperature corresponding to its maximum fatigue strength being called "peaking temperature" by Sinclair et al. [10].

We conducted our tests under medium cycle conditions and paid special attention to the convexity of the S-T (stress versus temperature) diagram and noticed how mild steel was influenced when it passed through the peaking temperature in the midst of a temperature variation. In our tests the temperature was varied in two or three steps from T_1 (nearly minimum fatigue strength at low temperature) going through the peaking temperature to T_2 (nearly the same strength at high temperature), then reversing the variation from T_2 to T_1. Under these temperature conditions fatigue tests were performed on SM41A† at a medium speed of 3400 rpm at temperature up to 500°C at a nominal constant stress amplitude.

In tests of temperature variations and stress amplitude of two levels, it has been difficult to express the entire results clearly because fatigue life is concerned with many factors, such as temperature, stress amplitude and hold-time. The authors offer a new method using the expressions $\log N_h/\log N_{500}$ versus n_2/N_2 in a single diagram.

*Yamaguchi University, Ube, Japan.
**Ube Technical College, Ube, Japan.
†the same as ASTM A 440-74.

FATIGUE TEST

Material Tested and Testing Procedure

The test material was SM41A as received from the factory, a rolled steel plate used for welding, 30 mm thick. Relevant details on chemical composition and mechanical properties are listed in Table I and Table II respectively. Figure 1 shows a sketch of the specimen's shape. Ono-type rotary bending fatigue machines were used, revolving constantly at 3400 rpm with the temperature ranging between R.T. and 800°C (controlled to ± 2°C).

The constant temperature fatigue tests were conducted at R.T., 150°C, 300°C, 400°C and 500°C. In the temperature variation fatigue tests, the following four models were used. In all the tests the specimens were continually subjected to a constant load.

Models of Temperature Variation

Four types of temperature variation were adopted: model A, B, C and D as shown in Figure 2. In model A the temperature was lowered rapidly and in model B the temperature was similarly raised in order to make the material pass through its peaking temperature during the changes. In model C the temperature was raised above peaking temperature and then lowered. In this model, the specimens were held at 150°C for the first 30 minutes. Model D was the same as model A, except that the initial temperature used was the peaking temperature. Hold-times are shown in Table III.

TEST RESULTS AND DISCUSSION

Test Results

"Constant temperature fatigue tests" were conducted by the methods outlined above. The results are shown in Figures 3 and 4. From these diagrams, it is clear that the peaking temperature of SM41A is about 400°C.

"Temperature variation fatigue tests" were conducted using the following expressions. n_1 and n_2 correspond to the number of cycles that were run at the first and second temperature, except in model C. In this model, n_1 and n_2 refer to the cycles run at the upper and lower temperatures respectively. N_1 and N_2 are the number of cycles to failure under the temperatures T_1 and T_2 as shown in Figure 5 respectively.

In model A, taking n_2/N_2 as absissa and $\log N_h/\log N_{500}$ as the corresponding ordinate, $\log N_h/\log N_{500}$ versus n_2/N_2 curves are shown in Figure 6, where N_h is the number of cycles corresponding to hold-time t_h at the first temperature T_1, N_{500} is the number of cycles to failure in 500°C, "constant temperature test". Thus, if we put the ratio $\log N_h/\log N_{500}$ is equal to α, α=1.0 corresponds to N_h=N_{500}, and $\alpha \to 0$ corresponds to N_h=N_{150}, that is, N_h nearly coincides with the number of cycles to failure in the 150°C "constant temperature test". By these procedures, when the temperature is changed, it becomes possible to express the relations between fatigue life, stress amplitude and hold-time (or number of cycles) with a single diagram constructed to clarify fatigue behaviour at each temperature.

Figures 7~9 are the diagrams constructed in this manner for models B, C and D. The figures in the diagrams indicate the values of n_1/N_1.

Discussion

For model A, B and C, n_2/N_2 was almost always greater than 1.0, that is, the fatigue life at the second temperature had been remarkably extended for all models, especially when using a lower stress. The maximum values of n_2/N_2 seems to arise at about $n_1/N_1 \fallingdotseq 0.1\sim0.3$ for the lower stresses and indicates that the maximum strengthening of materials by strain aging occurs at a relatively early stage of the first heating.

In model A (Figure 6), the lengthening of fatigue life at the second temperature T_2 was most remarkable. Although the fatigue life at both the upper and lower limits of temperature was shortest, the life at the second temperature was lengthened remarkably in comparison with 150°C "constant temperature test". We suggest that this lengthening resulted from a cyclic strain aging phenomenon in which small interstitial solute atoms (for example, N and C) are presumed to strengthen material by diffusing to new dislocation sites and reanchoring dislocations in the fatigue affected zones. This strengthening of the material seemed to occur on passing through the peaking temperature during the temperature decrease from the first temperature T_1 and was maintained even at the lower temperature T_2.

In Figure 7, the actual increase of life of model B at the second temperature T_2 was small compared with model A. We have explained this finding as follows: at the second temperature T_2 (500°C), with an increase of the difussion velocity of solute atoms a so-called "dragging stress"[14] was reduced, and as a result a softening of the material occurs [14].

In model C (Figure 8), for the first time, the material underwent strengthening by the model B type process with t_h = 30 min., then re-strengthened by the model A type process.

In model D (Figure 9), setting the first temperature is the peaking temperature, for the stress level s = 26 k_g/mm^2 an increase of life under the second temperature was remarkable compared with the stress level s = 28 and 30 k_g/mm^2.

Slip-Band and Hardness

Typical microstructures of the specimens under constant temperatures and varying temperatures are shown in Figure 10 (a)~(h). Under constant temperatures slip bands and etch pits arose most often at about 300°C, but at 500°C they were seldom found. Under varying temperatures large numbers were found in model D, in model A and C they were occasionally seen, and in model B they were rare.

Figure 11 (a)~(b) shows the electron micrographs of etch pits and slip bands in specimens of varying temperatures.

In Figure 12 the micro-hardness of model D, in which a great deal of etch pits and slip bands arose, is compared with model B in which they were rarely found.

CONCLUSIONS

In order to make material pass through the peaking temperature 400°C in the midst of "temperature variation fatigue test" of mild steel, we set up four models of temperature variation, that is: (A) 500°C → 150°C; (B) 150°C → 500°C; (C) 150°C → 500°C → 150°C; (D) 400°C → 150°C. Under these temperature conditions, fatigue tests were performed on SM41A and the results were brought to the following conclusions by means of a new method of the expression, $\log N_h/\log N_{500}$ versus n_2/N_2 diagrams.

1) For all the cases, the life at the second temperature (n_2/N_2) was lengthened remarkably in comparison with both 150°C and 500°C "constant temperature test".
2) The fatigue life at the second temperature in model A which has a decrease process of temperature was appreciably longer than in model B having an increase in temperature.
3) A large number of etch pits and slip bands were found in model D, in model A and C there were small numbers, and in model B they were seldom observed.
4) The micro-hardness of the specimen in model D, in which a great deal of etch pits and slip bands arose, was appreciably higher than that of model B, in which they were rarely found.

REFERENCES

1. TAIRA, S., KOTERAZAWA, R. and OHNAMI, M., J. JSMS., 9, 1960, 636.
2. KATŌ, N., Trans. JSME., 27, 1961, 410.
3. TAIRA, S., MURAKAMI, Y. and KOTERAZAWA, R., Trans. JSME., 25, 1959, 1070.
4. BERRY, J. W., NASA MEMO, 11-21-58W, 1958, 20.
5. ANDŌ, Z., KATŌ, Y. and NAKANO, N., J. JSMS., 11, 1962, 379.
6. DUNSBY, J. A., Proc. ASTM., 65, 1965, 736.
7. МАЛЫКЕВИЧ, А. В., МАРИНЕЙ, Т. К. and РАХМАН, В. М., Изв Вест Вуз, МАШИНОСТР., 12, 1964, 39.
8. KATŌ, Y. and HIROSE, M., JSSFM., 5, 1970, 115.
9. HIROSE, M., KATŌ, Y. and HASEGAWA, N., J. JSMS., 23, 1974, 777.
10. LEVY, J. C. and SINCLAIR, G. M., Proc. ASTM., 55, 1955, 866.
11. TAIRA, S., FUJINO, M., SAKON, T. and MATSUDA, Y., J. JSMS., 22, 1973, 242.
12. SHIMIZU, S., MOCHIZUKI, T. and FUJIMITSU, T., Preprint of JSME., No. 735-1, 1973, 41.
13. SHIMIZU, S., MOCHIZUKI, T. and FUJIMITSU, T., Preprint of JSME., No. 745-1, 1974, 41.
14. SUTŌ, H., J. JSMS., 21, 1972, 159.

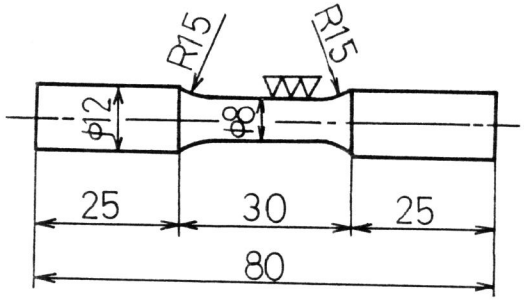

Figure 1 Test specimen

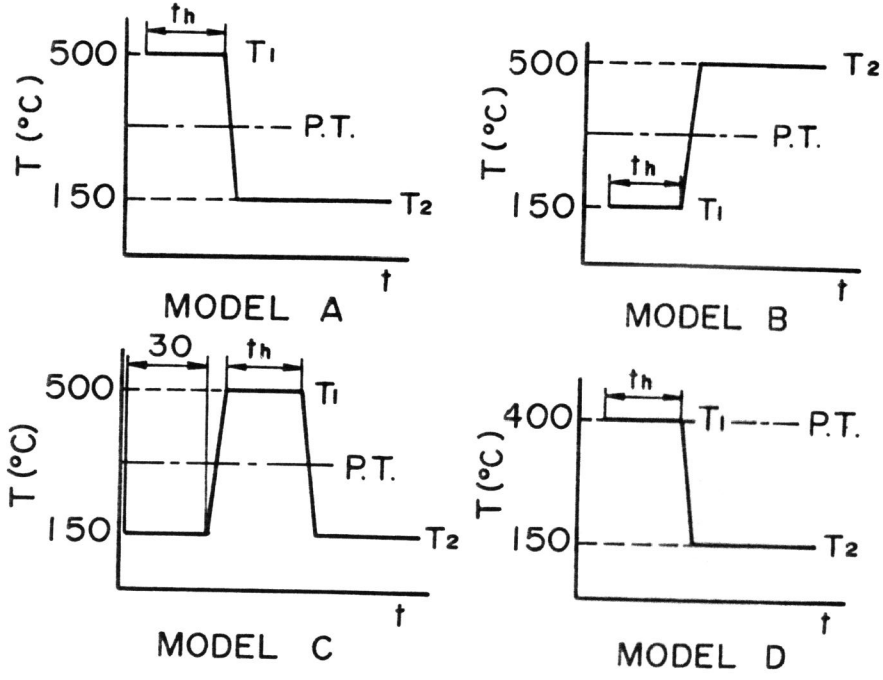

Figure 2 Models of variation of temperature

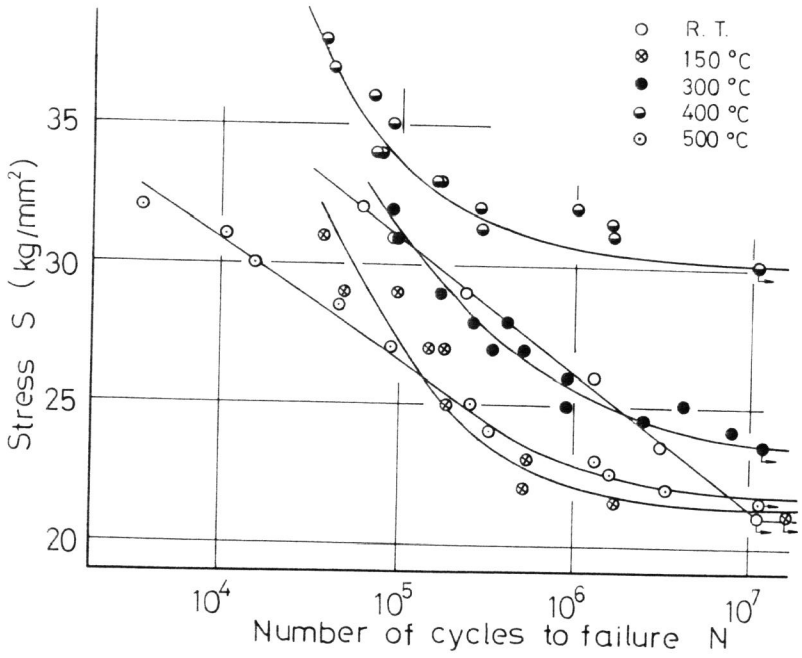

Figure 3 S-N curves of SM41A (as received) at R.T., 150°C, 300°C, 400°C and 500°C

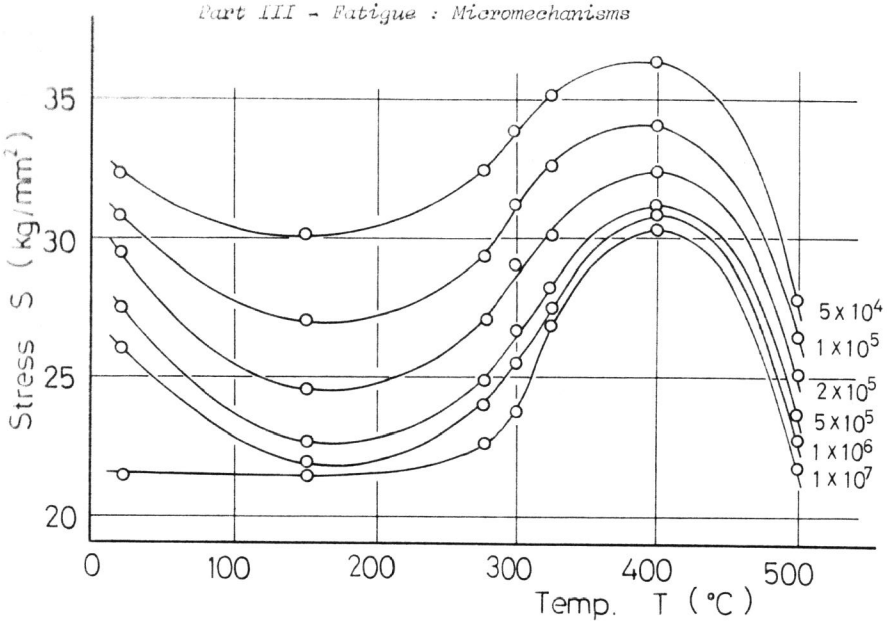

Figure 4 Temperature-repeated stress diagram with endurance strength as a parameter (for SM41A)

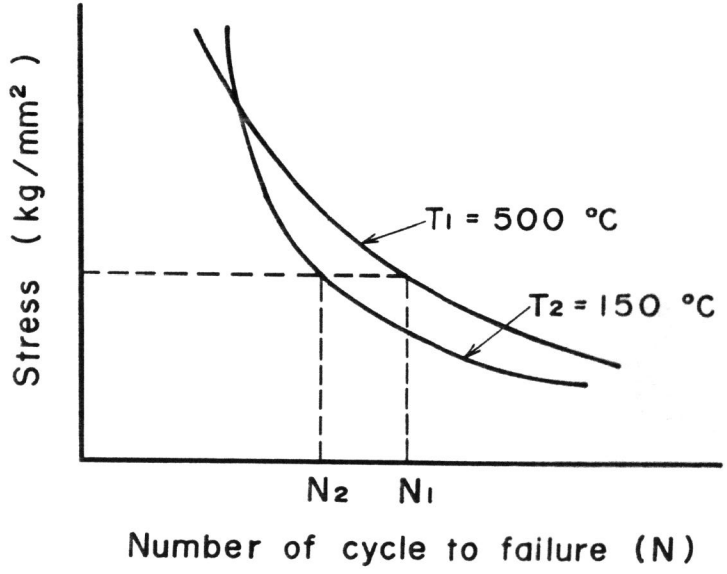

Figure 5 N_1, N_2 corresponding to the temperature T_1 and T_2.

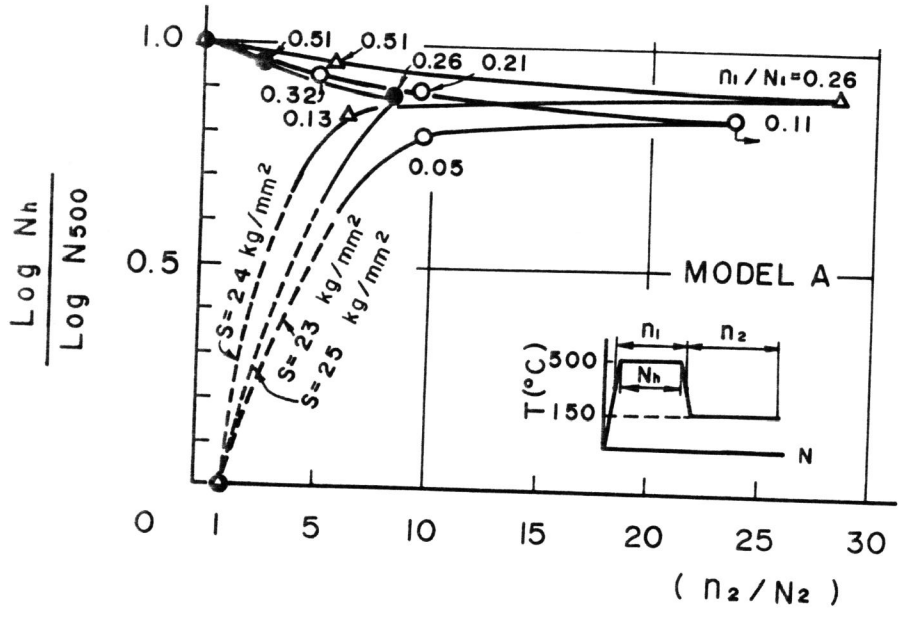

Figure 6 Log N_h/log N_{500} versus n_2/N_2 curves of model A

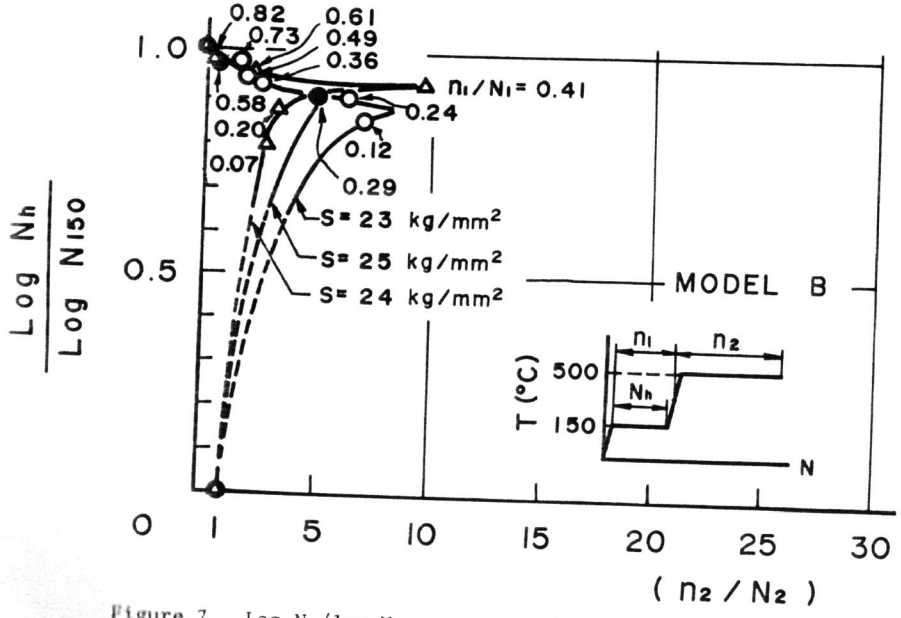

Figure 7 Log N_h/log N_{150} versus n_2/N_2 curves of model B

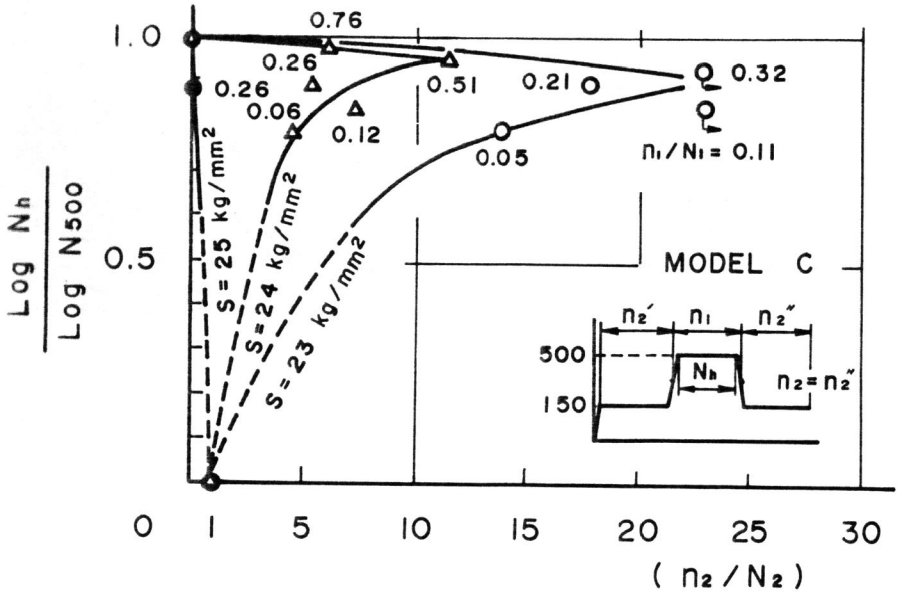

Figure 8 Log N_h/log N_{500} versus n_2/N_2 curves of model C

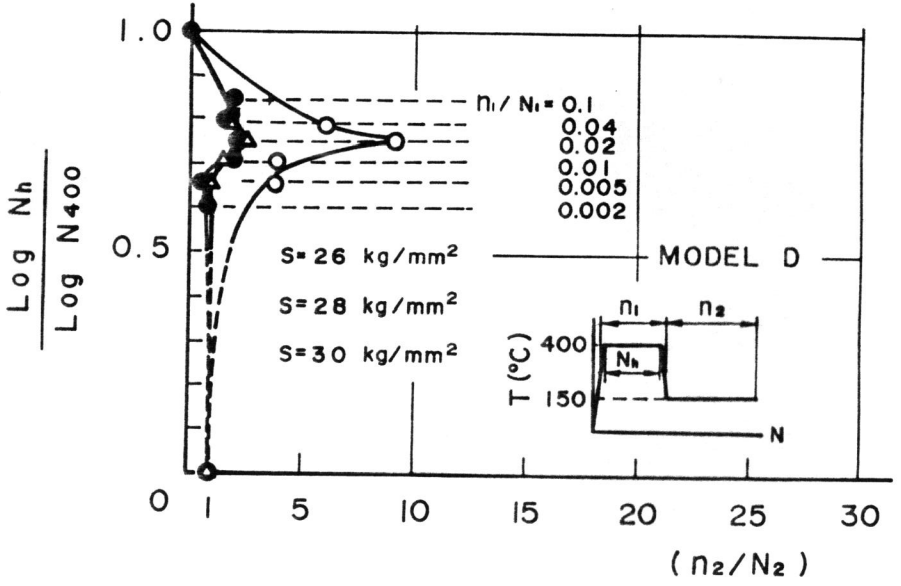

Figure 9 Log N_h/log N_{400} versus n_2/N_2 curves of model D

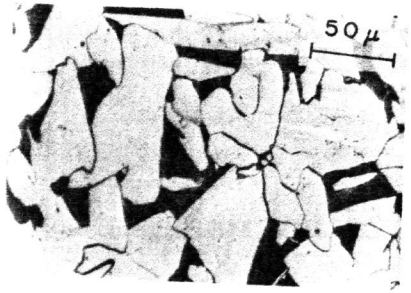

(a) R.T.
S = 31 kg/mm^2
N = 0.0913 × 10^6

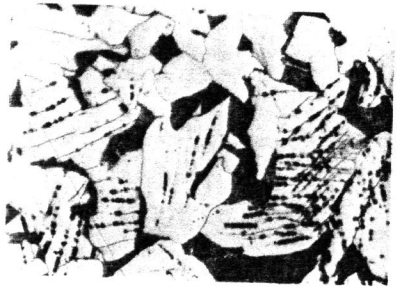

(b) T = 300^{0}C
S = 31 kg/mm^2
N = 0.0947 × 10^6

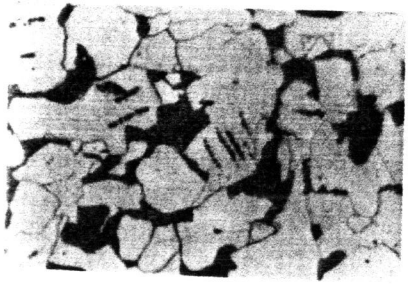

(c) T = 400^{0}C
S = 31 kg/mm^2
N = 1.5908 × 10^6

(d) T = 500^{0}C
S = 31 kg/mm^2
N = 0.0107 × 10^6

Figure 10 Typical microstructures of specimens under constant temperatures and varying temperatures

(Figure 10 continued)

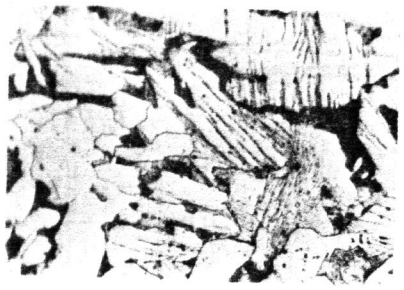

(e) MODEL A
S = 24 kg/mm^2 t_h = 30 min
N = 7.2471 × 10^6

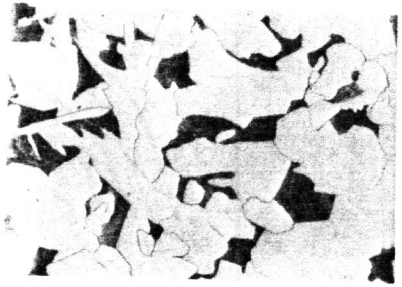

(f) MODEL B
S = 24 kg/mm^2 t_h = 30 min
N = 3.9985 × 10^6

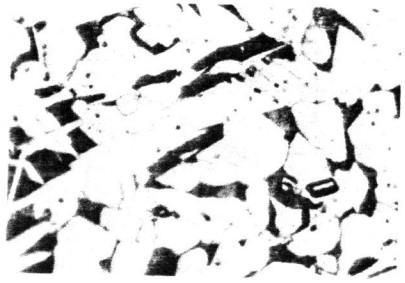

(g) MODEL C
S = 24 kg/mm^2 t_h = 30 min
N = 1.7359 × 10^6

(h) MODEL D
S = 30 kg/mm^2 t_h = 15 min
N = 0.1381 × 10^6

Figure 10 Typical microstructures of specimens under constant temperatures and varying temperatures.

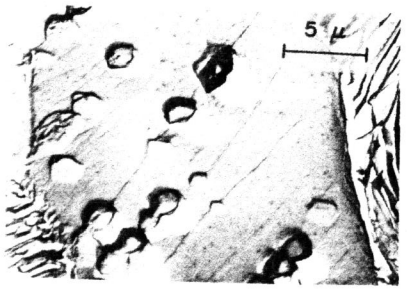

(a) MODEL D
S = 30 kg/mm^2 t_h = 15 min
N = 0.1381 × 10^6

(b) MODEL B
S = 24 kg/mm^2 t_h = 30 min
N = 3.9985 × 10^6

Figure 11 Etch pits and slip bands in electron micrographs of specimens under constant temperatures and varying temperatures.

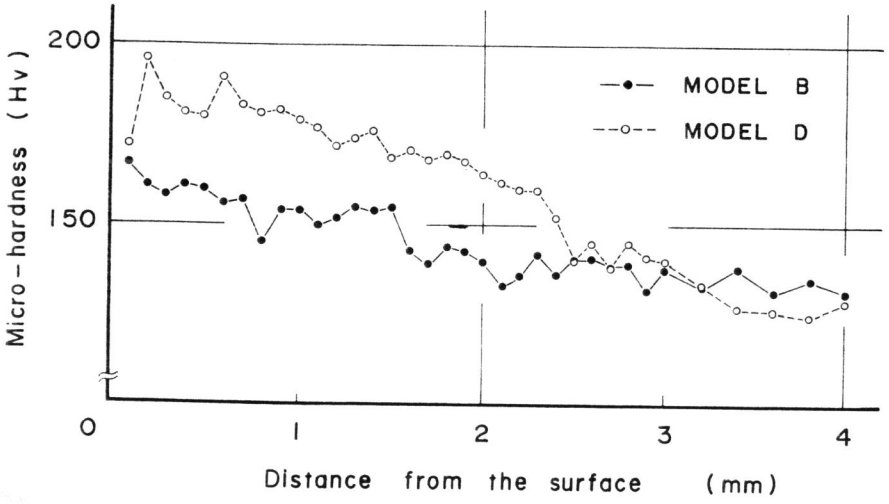

Figure 12 Comparison of micro-hardness between model D and model B.

Table I Chemical compositions of material

Material	Symbol	Chemical compositions (%)				
		C	Si	Mn	P	S
Rolled steel for welded structure	SM41A	0.150	0.210	0.650	0.013	0.014

Table II Mechanical properties of material

Symbol	Yield stress (kg/mm^2)	Ultimate strength (kg/mm^2)	Elongation (%)
SM41A	29.0	45.0	30.0

Table III Numerical values of hold-time

Time / Symbol / Model	t_h (min)					
	a	b	c	d	e	f
A	15	30	60	90	—	—
B	5	15	30	45	60	90
C	7	15	30	60	90	—
D	7	15	30	60	120	300